Trends in South Pole Particle Concentrations Imply Holocene Westerly Wind Strengthening

Aaron Chesler[1,2,*], Dominic Winski[1,2], Karl Kreutz[1,2], Bess Koffman[3], Erich Osterberg[4], David Ferris[4], Zayta Thundercloud[4], Jihong Cole-Dai[5], Mark Wells[6], Aaron Putnam[2], and Katherine Anderson[4]

[1]Climate Change Institute, University of Maine, Orono, Maine, 04469, USA
[2] School of Earth and Climate Sciences, University of Maine, Orono, Maine, 04469, USA
[3]Department of Geology, Colby College, Waterville, Maine, 04903, USA
[4]Department of Earth Science, Dartmouth College, Hanover, New Hampshire, 03755, USA
5Department of Chemistry and Biochemistry, South Dakota State University, Brookings, South Dakota, 57007
[6]School of Marine Sciences, University of Maine, Orono, Maine, 04469, USA
*now at: Environmental Studies and Science Program, Colorado College, Colorado Springs, 80903, USA

Correspondence to: Aaron Chesler (aaron.chesler@maine.edu)

Abstract. The Southern Hemisphere Westerly Winds (SHWW) play an important role in global climate and Antarctic ice sheet dynamics; however, high-resolution proxy reconstructions are sparse. Conflicting evidence suggests SHWW latitudinal change weakening and/or strengthening throughout the Holocene. Dust microparticles preserved in Antarctic ice cores provide valuable paleo-perspectives on SHWW behavior. We present South Pole Ice Core (SPC14) dust records spanning the Holocene. Dust concentrations (1.1 – 5.1 μm) decrease through the Holocene, while the coarse particle percentage (CPP) increase due a relatively larger decrease in finer (1.1 – 3.2 μm) dust. Dust trends, CMIP6-PMIP4 model results, and SH proxy records are consistent with an increase in wind speed south of the SHWW core (>~51°S) across the mid-Holocene. The decrease in dust concentration may reflect weakening winds coupled with precipitation and/or vegetation changes over mid-latitude dust source regions, while the CPP increase may indicate strengthening of the SHWW south of the core. Our findings suggest that following a stable early Holocene, the SHWW began contracting towards Antarctica ~7 – 6 ka.

1 Introduction

The Southern Hemisphere Westerly Winds (SHWW) represent the strongest persistent surface wind system on Earth. Variations in the SHWW influence global carbon cycling and heat distribution, and are believed to play a critical role in Earth's climate and ice sheet stability across wide-ranging timescales (Hillenbrand et al., 2017; Russell et al., 2006). The strength and latitudinal position of the SHWW during the past several centuries is related to changes in the equator-to-pole temperature gradient (i.e., Perren et al., 2020). During warm periods, SHWW migrate southward and increase in strength and during cooler periods migrate northward and weaken. Increases in SHWW strength intensify the ocean-to-atmosphere transfer of CO_2 via upwelling and impact ice sheet stability and mid-latitude vegetation/precipitation dynamics (Hillenbrand et al., 2017; Anderson et al., 2009; Toggweiler and Russell, 2008; Moreno et al., 2010). However, while the SHWW are an important climatic feature, Holocene SHWW dynamics are poorly constrained, with previous work disagreeing between zonally symmetric or asymmetric change in the strength and/or intensity as well as the mean latitudinal position of the winds (Saunders et al., 2018; Perren et al., 2020; Moreno et al., 2010; Hillenbrand et al., 2017; Van Der Bilt et al., 2022; Zwier et al., 2022; Varma et al., 2012).

Microparticle records of concentration and relative particle size (i.e., coarse particle percentage; CPP) from Antarctic ice cores offer a unique perspective of SHWW strength and/or position dynamics because they have been interpreted to reflect source-to-sink conditions and atmospheric variability, specifically distillation (Markle et al., 2018), geomorphology of the source regions (Sugden et al., 2009), wind strength (Koffman et al., 2014) vegetation cover, precipitation (Tegen and Schepanski, 2018), and atmospheric transport patterns (Albani et al., 2018; Delmonte et al., 2020; Delmonte et al., 2013;

Delmonte et al., 2002; Aarons et al., 2019; Aarons et al., 2017; Aarons et al., 2016; Koffman et al., 2023). However, there are few complete Holocene dust records from Antarctica, limiting a full interpretation of past SHWW behavior. Here we measure and develop records of dust concentration and CPP in the South Pole Ice Core (SPC14) to better constrain Holocene SHWW dynamics. The South Pole is well-situated because of its geographic position, which facilitates hemispheric-scale interpretations, the relatively high snow accumulation rate that adds precision to the time record, and the 60 years of aerosol and meteorological studies in the region (Lazzara et al., 2012; Sheridan et al., 2016; Clem et al., 2020; Casey et al., 2014).

2 Methods

We measure microparticle concentration and size distributions using a subset of data collected from a continuous flow analysis (CFA) Klotz Abakus laser dust sensor at Dartmouth College (Text S1; Breton et al., 2012; Winski et al., 2021; Osterberg et al., 2006). We analyze particles ranging from 1.1 – 5.1 µm and limit our temporal analysis from 11300 years BP to 250 years BP. Uncertainty during the Holocene is ± 18 years while between 1800 – 3100 years BP the uncertainty increases to ± 25 years (Winski et al., 2019). There while the CFA can produce sub-annual resolution, we resample the data using the median value to 50-year intervals. To facilitate a comparison with other ice core records, we use a density of 2.6 g cm^{-3} (following Koffman et al., 2014) and a spherical shape to estimate flux, rather than the measured prolate particle shapes (Chesler et al., 2023). While we recognize that South Pole particle shape metrics (i.e., mass and flux) are unconstrained for the Holocene (i.e., Chesler et al., 2023) because of limited available data, we use South Pole flux as a comparison tool to assess similarities between other available microparticle Antarctic Holocene. We restrict particle metrics to number concentration and CPP because the particle shape assumption (i.e., particle flux and mass concentration), can artificially increase particle metric concentrations by 25 – 44%. We use a spherical particle shape assumption to facilitate comparison to other Antarctica ice core particle records that include a volume assumption (i.e., flux) using particles that range between 1.1 – 5.1 µm due to the particle number concentration distribution (Figure 1e). We use particle number concentration measured between 1.1 – 5.1 µm and CPP (defined as number of particles mL^{-1} [3.2 – 5.1] /[1.1–5.1] µm diameter x 100) following other East Antarctic studies due to the similarity of the South Pole particle flux to other East Antarctic core records (Figure 1e; i.e., Delmonte et al., 2020). While this produces higher-than-realistic particle flux values, it mitigates discrepancies from comparing dissimilar metrics, whereas in the past particle shape has been assumed to be spherical (Chesler et al., 2023; Simonsen et al., 2018; Potenza et al., 2016). Studies concerned with the absolute magnitude of dust flux at the South Pole should use prolate particle shapes to calculate flux (Chesler et al., 2023; data at USAP-DC, DOI: 10.15784/601553). 2.1 HYSPLIT and CMIP6 models

We ran HYSPLIT NCEP trajectories for December, January, February (austral summer; DJF) and June, July, August (austral winter; JJA) from 1980 – 2022 (inclusive) hourly for 10 days over a 90-day period.

We run the model at an altitude of 1000 m following Schwanck et al. (2017) and use the default vertical motion for the model. We then calculate air mass origin percentage using a 2 x 2° grid to identify where air masses originate 10 days prior to reaching the South Pole. We also explore changes in atmospheric temperature, wind speed, and precipitation using CMIP6 – PIMP4 model outputs. We use 11 different models (Table 1) to assess model agreement between mid-Holocene runs (6,000 years ago) relative to pre-industrial control (piControl). We calculate model difference by subtracting the mid-Holocene from pre-industrial to assess change in each climate variable from the mid-Holocene to the pre-Industrial. We replace all positive values with a value of 1, which signifies an increase with time, and replace all negative values with a 0 and sum all model runs. Our method allows us to assess if the models agree to an increase/decrease in each climate variable rather than assessing the magnitude of change between each model.

Table 1: List of CMIP6-PMIP4 Models used with name, institution, resolution using the r1i1p1 (r = realization, i = initialization, p = physics, respectively) ensemble, with variables for surface temperature (tas), precipitation, (pr), and surface wind speed (sfc Wind).

Model	Institute	Time Resolution	Grid Size		Model Run Time		Variables
			Latitude (°)	Longitude (°)	mid-Holocene	piControl	
ACCESS-ESM 1-5	Commonwealth Scientific and Industrial Research Organization, Australia	Amon	1.25	1.88	501 - 800	101 - 0600	pr, tas
AWI-ESM-1-1-LR	Alfred Wegner Institute, Germany	Amon	1.85	1.88	3106 - 3205	1850 - 1954	pr, sfcWind, tas
FGOALS-f3-L	Chinese Academy of Sciences, China	Amon	1	1.25	720 - 1219	600 - 1160	pr, sfcWind, tas
GISS-E2-1-G	Goddard Institute for Space Studies, USA	Amon	2	2.5	2900 - 3199	4150 - 5000	pr, sfcWind, tas
INM-CM4-8	Institute for Numerical Mathematics, Russian Academy of Science, Russia	Amon	1.5	2	1880 - 2079	1850 - 2380	pr, sfcWind, tas
IPSL-CM6A-LR	L'Institut Pierre-Simon Laplace, France	Amon	1.27	2.5	1850 - 2399	1850 - 2349	pr, sfcWind, tas
MPI-ESM1-2-LR	Max Planck Institute for Meteorology, Germany	Amon	1.85	1.88	1001 - 1500	1850 - 2849	sfcWind
MRI-ESM2-0	Meteorlogical Research Institute, Japan	Amon	1.11	1.13	1951 -2150	1850-2550	pr, sfcWind, tas
NCAR - CESM2	National Center for Atmospheric Research, USA	Amon	0.94	1.25	0 - 700	1 - 1200	pr, sfcWind, tas
NUIST - NESM3	Nanjing University of Information Science and Technology, China	Amon	1.875	1.875	1798 - 1897	500 - 0999	pr, tas
NorESM2-LM	Norwegian Climate Centre	Amon	1.875	2.5	2101 - 2200	1600 - 2100	pr, tas

3 Results

Total dust number concentrations (i.e., 1.1 – 5.1 µm # particles mL^{-1}) make up on average ~85 – 96% of all particles measured (median ± 1σ; Figure 1). The total dust number concentration and CPP abundance have opposing trends, yet the timing of change in both trends begins about ~7000 years BP. This inverse relationship is most apparent during the mid-Holocene (~7000 – 3000 years BP).

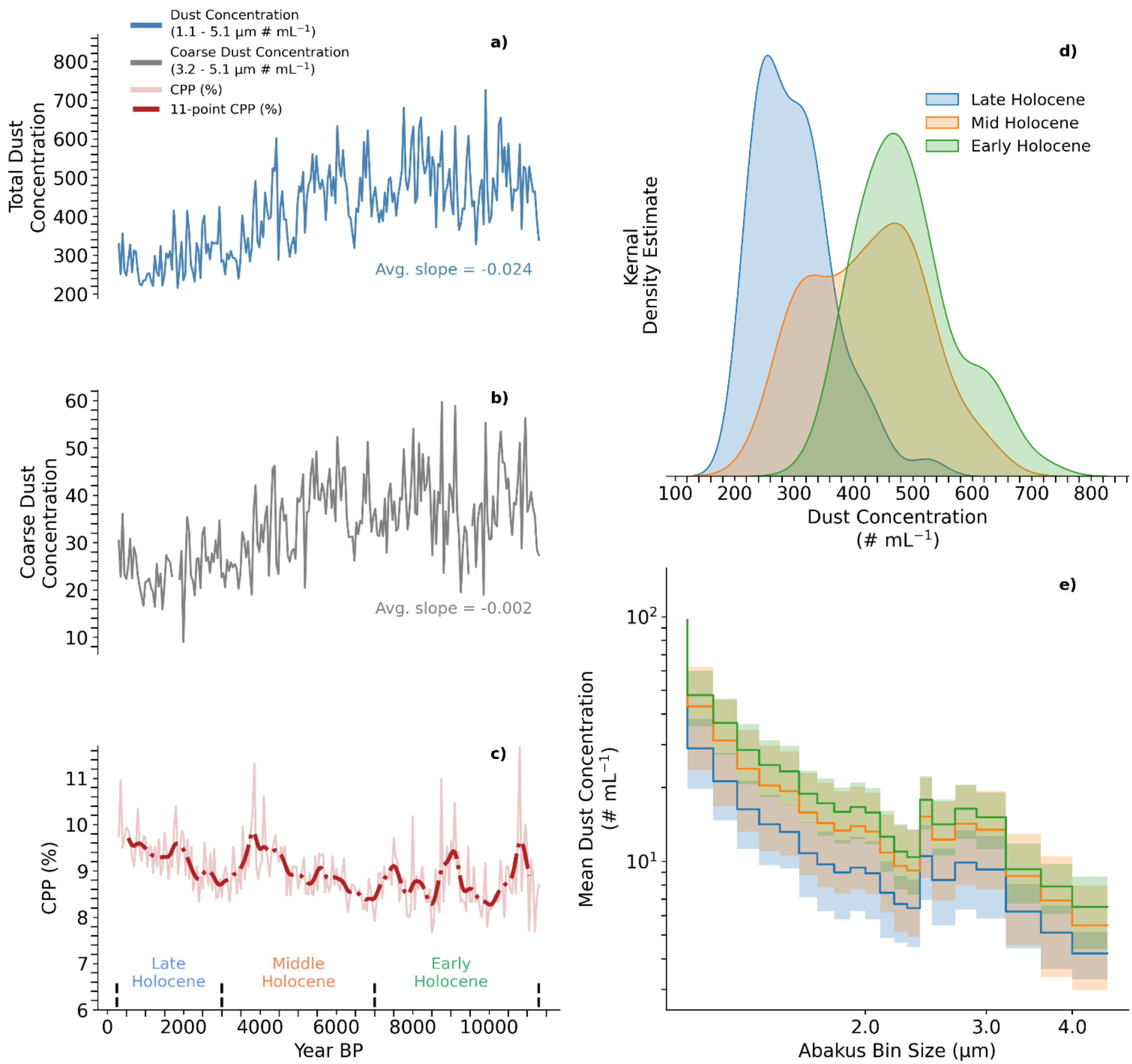

Figure 1a – e: 1a) 50-year median resampled SPC14 dust concentration (1.1 – 5.1 µm # particles mL^{-1}; blue line), 1b) coarse particles (3.2 - 5.1 µm # particles mL^{-1}; grey line), 1c) 50-year median resampled CPP (light red) and CPP 11-point rolling Gaussian mean (2σ; red dashed line), 1d) total dust # particles mL^{-1} concentration distributions, and 1e) total dust # particles mL^{-1} size distributions by time period. The figure is limited to 11,300 – 250 years BP to highlight Holocene variability recorded in the South Pole annually resolved record. Inset shows histograms of dust concentration from each of the three time periods highlighted in the record. Note the bimodal distribution during the mid-Holocene highlighting the transition from early to late Holocene. Average median absolute deviation (MAD) for the particle concentration is ~84 (Figure S1).

3.1 Holocene dust flux

South Pole Holocene dust flux has a similar magnitude and trend to other Antarctic plateau ice core sites (50-year resampled), with a median flux of 0.45 ± 0.23 mg m^{-2} yr^{-1} (2σ; Figure S1). The SPC14 Holocene median dust flux is within 2σ of the EPICA Dome C (0.33 ± 0.23) and Vostok dust flux records (0.63 ± 0.21), while non-plateau sites (i.e., TALDICE [~1.31 mg m^{-2} yr^{-1}] and WAIS Divide [~1.36 mg m^{-2} yr^{-1}; particles <5.1μm]) are significantly higher (Koffman et al., 2014; Albani et al., 2012; Lambert et al., 2012; Petit et al., 1990). NOAA HYSPLIT analysis from austral summer (DJF) and winter (JJA; 1980 – 2022) highlights an Atlantic sector signal (Figure 2; Rolph et al., 2017; Stein et al., 2015). Previous South Pole dust analyses identified a primary austral summer peak (Lazzara et al., 2012; Carrasco et al., 2003; Parungo et al., 1981; Hogan et al., 1984; Bodhaine et al., 1986). Our HYSPLIT analysis identifies 10-day air mass origin locations during the summer with an average coordinate of 70.9 ± 9.4° S -1.4 ± 80.03° W, indicating a primarily Weddell Sea/Atlantic Sector modern signal. Following Albani et al. (2012), we compare our Holocene dust flux record against $\delta^{18}O$ to assess a primarily remote or mixed dust source. Albani et al. (2012) compared the TALDICE dust-$\delta^{18}O$ profile against EPICA Dome C as EPICA Dome C is considered to represent remote dust sources. We define remote dust sources similarly, as those from the mid-latitudes (i.e., southern South America and Australia; Delmonte et al., 2020), local sources from Antarctica (i.e., Aarons et al., 2019), and mixed being a combination of the remote and local. The Holocene South Pole dust record and $\delta^{18}O$ have a weak significant relationship (r = -0.17, p = <0.01), which suggests a primarily remote dust source signal. Albani et al. (2012) interpreted the close relationship between dust and $\delta^{18}O$ trends at Talos Dome as evidence of a local/regional climate influence. Conversely at Dome C during the Holocene, the dust and $\delta^{18}O$ did not vary proportionally, which is interpreted to reflect mid-to-high latitudinal processes (Lambert et al., 2008; Albani et al., 2012). The similarity to other East Antarctic sites (i.e., Dome C and Vostok; Figure 2), modern HYSPLIT back-trajectory modelling (Figure 3), and internal dust-water isotopes relationships suggests that the South Pole represents a site typical of Antarctic plateau locations, with dust likely sourced from remote region, facilitating comparisons (Figure S1 and 2).

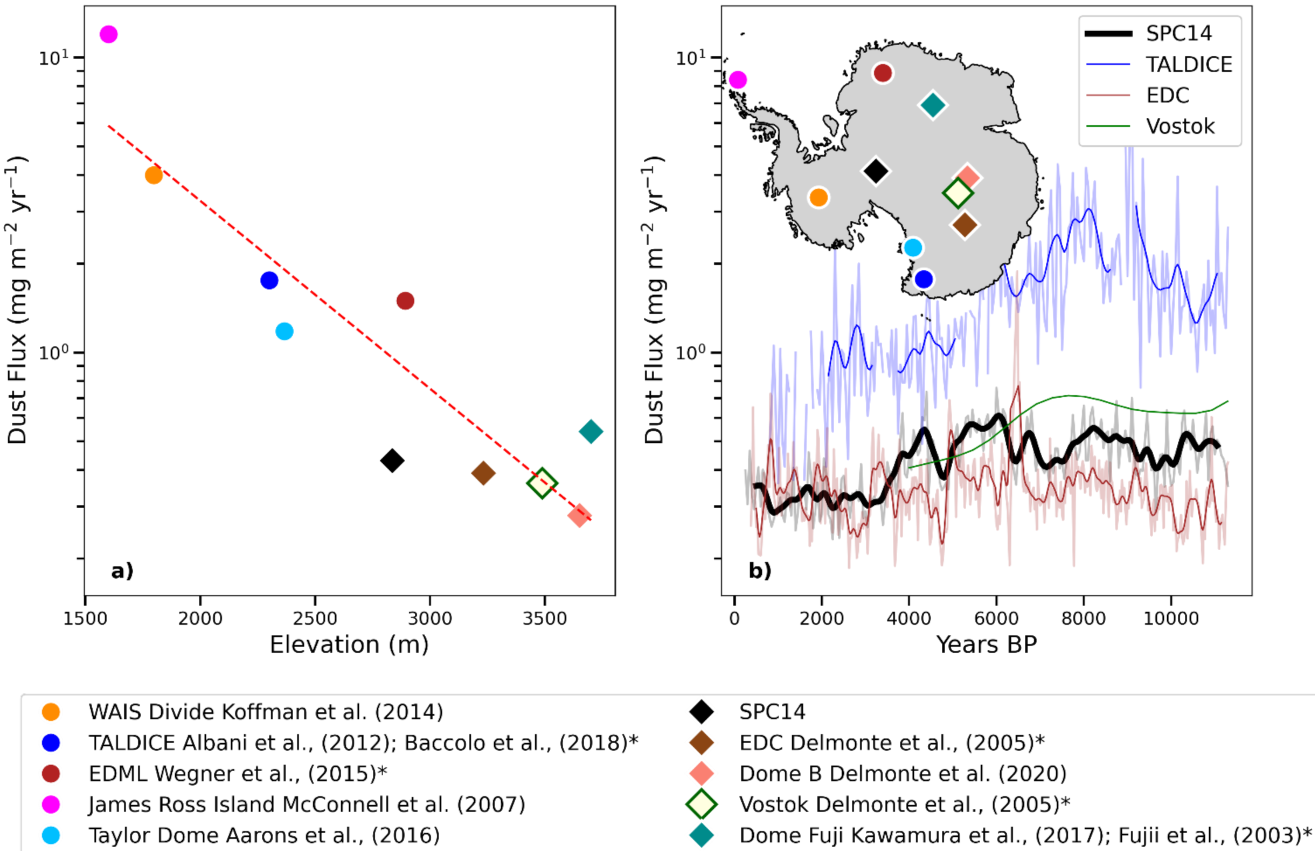

Figure 2a and b: Comparison of SPC14 dust metrics with other Antarctic Holocene records. Plateau sites are depicted with diamonds while non-plateau (i.e., WAIS and coastal locations) are depicted with circles. Labels containing a * symbol at the end were reported in (Delmonte et al., 2020). In S1a, SPC14 dust flux is similar to other cores based on drill site elevation. S1b shows available Holocene flux records from Talos Dome fine particle flux (0.6 – 5 μm mg m^{-2} yr^{-1}) (Albani et al., 2012), Vostok (Petit et al., 1990), EPICA Dome C (EDC; Lambert et al., 2012). SPC14 dust flux is similar to other East Antarctic sites (Vostok and EDC) and is on average ~67% lower compared to TALDICE. TALDICE, SPC14, and EDC were resampled to 50-year median values (background variability), and the darkened lines are the 11-point rolling gaussian mean for TALDICE, SPC14, and EDC.

3.2 Holocene trends in dust deposited at the South Pole

The SPC14 dust concentration decreases relatively linearly during the Holocene by an average of ~20 particles mL^{-1} kyr^{-1} (Figure 1; Table S1). To describe the SPC14 dust record, we divide the Holocene into early (11,300-7,000 years BP), middle (7,000-3,000 years BP) and late (3,000 - 250 years BP) periods. During the early Holocene, dust concentration remained relatively stable, followed by a nearly two-fold decrease to the modern era (Table S1). Dust concentration distributions in all three time periods are statistically different (Figure 1 inset; p-value < 0.01; Table S2a), further supporting a reduction in Holocene dust deposition.

Coarse particle concentrations have a similar decrease compared to the fine particles, however, at an order of magnitude smaller (total dust concentration slope = ~ -20 # particles mL^{-1} kyr^{-1} compared to coarse particle decrease ~ -2 # particles mL^{-1} kyr^{-1}. The total and coarse particle fractions have similar albeit slightly different changes throughout the Holocene, whereas there is a ~ -40% difference between the Early Holocene and Late Holocene for total dust concentration and a ~ -35% difference between the Early Holocene and Late Holocene for coarse dust concentration. This 5% difference results in an increase in the CPP starting at ~7000 years BP. In contrast, CPP increases over the Holocene from 8.6% to 9.4%. The CPP during the early and late Holocene are distinct, with significantly different distributions (two-sided t-test; p-value < 0.01; Table S2b). The increase in CPP is driven primarily by a steeper decrease in fine particles (1.1 – <3.2 µm) rather than an increase in coarse particles. Although the coarse dust concentration also decreases slightly throughout the Holocene, the decrease is much less than that of the total dust concentration slope such that the proportion of coarse particles rises, especially during the middle Holocene. CPP has a weak statistical relationship with dust concentration during the Holocene (Spearman r = -0.28; p < 0.01), suggesting independent factors driving most of their variability. During the late Holocene, both the dust concentration and CPP have the lowest variability compared to the middle or early Holocene (Figure 1, Table S1).

3.3 Modern air mass sources

Our HYSPLIT results (Figure 2) identify a high percentage of 10-day air mass origins in the Weddell, Dronning Maud Land, Enderby and Kemp Land (i.e., Atlantic Sector) during DJF. During JJA, air masses at their 10-day origin are more latitudinally and longitudinally diverse, with a greater percentage of air mass origins over the Atlantic and Pacific sectors of the Southern Ocean (Figure 3c and d).

4 Discussion

4.1 Dust source(s)

The South Pole receives air masses from multiple different regions, including Western Antarctica (Nicolas and Bromwich, 2011), the Weddell Sea (Winski et al., 2021; Lazzara et al., 2012; Arimoto et al., 2008), and downslope from the East Antarctic Plateau (Lazzara et al., 2012). The dominant advection of remote air masses are from Weddell Sea and WAIS with a minor source from EAIS (Harris, 1992).Our HYSPLIT data analysis then is reflective of past studies and highlights modern seasonal latitudinal changes in wind strength and position of 10-day air mass origins. While we recognize that some air masses and dust particles can be sourced from the East Antarctic Plateau, this area would not be the primary source of reduced dust emission during the mid-Holocene since southern South America and Australia are the primary sources of dust during the Holocene and modern period (Wegner et al., 2012; Vecchio et al., 2024; Delmonte et al., 2020). Rather we suggest that the decrease in dust concentration was driven by reduced SHWW activity in the wind in the mid-latitudinal regions (Figure 4). Because the fine particles decrease significantly during the mid-Holocene compared to the relatively small decrease in the total number of coarse particles, we explore the possibility of different sources of fine vs coarse particles. Given the multiple trajectories of air masses to the South Pole, we do not specify a specific dust source contributor but rather limit our interpretation to local or remote dust sources.

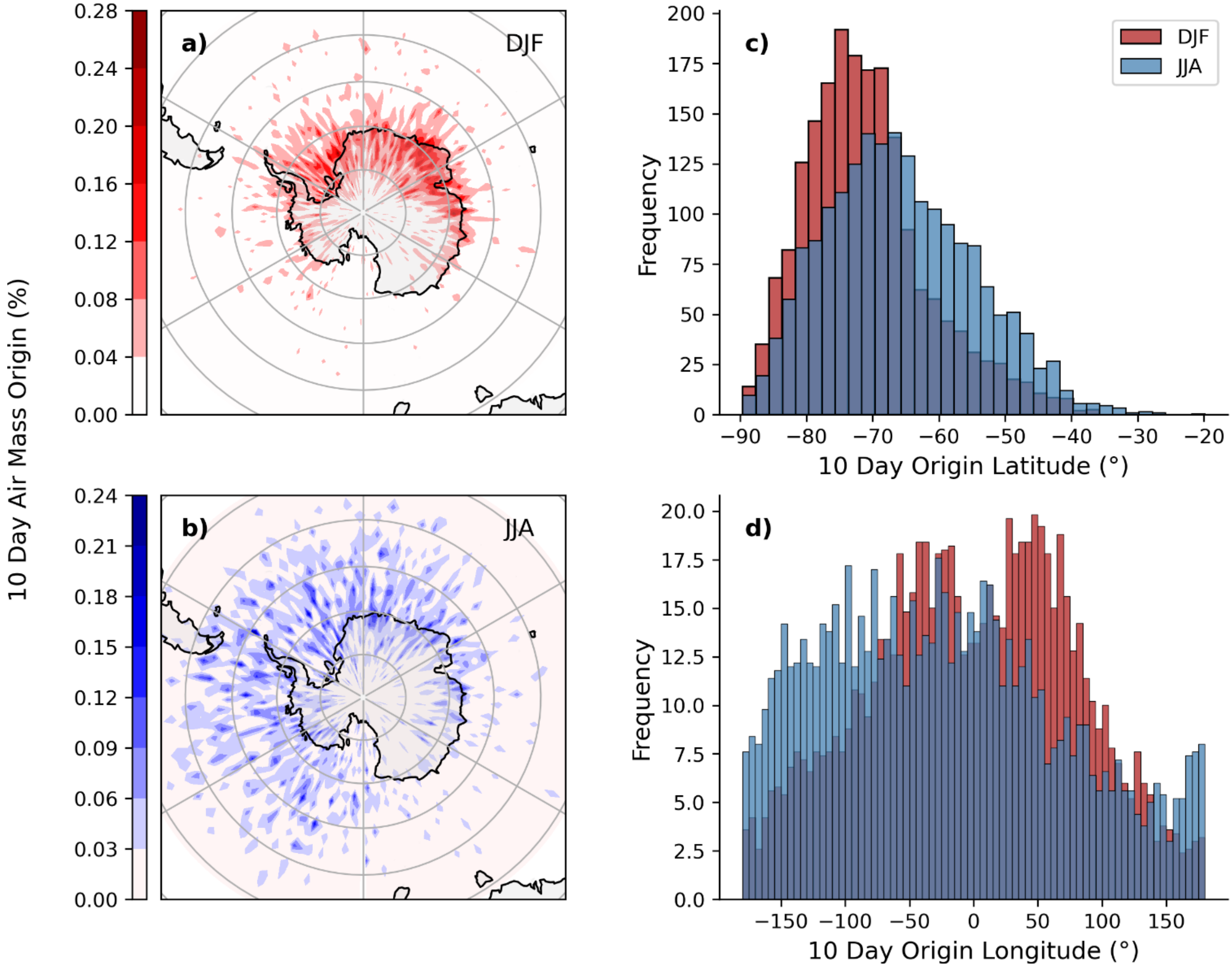

Figure 3a - d: NOAA HYSPLIT analysis of 10-day hourly back-trajectory of air masses to the South Pole from 1980 – 2020 (Rolph et al., 2017; Stein et al., 2015). Height elevation of back trajectory is 1000m. 3a and b indicate the percentage of 10-day air masses (240 hour) in a 2x2° grid. 3c and d are histograms of frequency of seasonal data by latitude and longitude, respectively.

4.2 Proxy and modelled Holocene wind changes

We suggest that the SPC14 dust concentration and CPP records indicate a mid-to-high latitude (>~51°S) strengthening and southward shift of the SHWW during the mid-Holocene (~7000–3000 y BP), consistent with other proxy-based reconstructions of SHWW migration and CMIP6-PMIP4 model output (Figure 4a). Simulations from an ensemble of CMIP6-PMIP4 models (Table 1; Figure 4), all show a clear pattern of decreased surface wind strength over South American and mid-latitude (40°–50°) oceans concurrent with increasing surface wind strength over the Antarctic periphery between the mid-Holocene (6,000 BP) and pre-Industrial (piControl; Figure 4). The weakening of the SHWW over latitudes >~51°S is consistent with the observed decrease in the SPC14 dust concentration, indicating a reduced entrainment of fine remote dust sources in surface winds. We note broad agreement spatially with Southern Hemisphere temperature and precipitation increase between the mid-Holocene and historical periods over common dust source regions (i.e., South America, Australia, and Antarctica; Figure 4). A southward shift in the core of the SHWW can simultaneously explain the opposing trends in CPP and total particle concentration at the South Pole while being consistent with proxy records reflecting changes in winds, precipitation and/or glacier retreat across the mid-to-high-latitude Southern Hemisphere during the mid-Holocene.

Furthermore, we also compare our dust number concentration results using Osman et al. (2021) surface air temperature record throughout the Holocene (11300 – 100 years ago) from the Western and Eastern Pacific Ocean 30 – 55°S similarly to Lamy et al. (2010) to assess temperature (wind) gradients (Figure S2). We find that average temperature gradients steepen, which we interpret to reflect a strengthening of the winds throughout the Holocene. Statistically, the dust concentration record has a significant anticorrelating relationship to both temperature gradients (p-value < 0.01) for both the western and eastern mid-latitudinal Pacific Ocean. However, the South Pole dust concentration has a stronger anticorrelating relationship to the western Pacific Ocean compared to the eastern Pacific Ocean ($r = -0.76$ and -0.65, respectively). We interpret this relationship to reflect changes in the Westerly Winds shifts and warm water circulation into the south Pacific gyre described in Denton et al. (2021). The small variations between the Western and Eastern Pacific further suggest asymmetrical wind changes, which support the conclusions of Lamy et al. (2010), Kaplan et al. (2016) with a cooling of coastal South American temperatures throughout the Holocene, and support increased upwelling in Pine Island Bay during the early Holocene Hillenbrand et al. (2017).

More northern proxy records corroborate a poleward shift in the SHWW during the mid-Holocene. Lacustrine sediments from Emerald Lake, Macquarie Island (~55°S, ~159°E) reflect a weakening of the SHWW between 11200 – 9200 years BP, followed by a period of increased variability between 9200 – 5300 years BP, and sustained and strengthened winds between 5300 – 200 years BP (Figure 5f; Saunders et al., 2018). In southern South America, Moreno et al. (2010), compared changes in precipitation via plant community changes in two lacustrine records (Lago Guanaco and Lago Condorito; 51°

[Figure 5e] and 41°S, respectively, ~72°W). Their results show a relatively dry period during the Early Holocene between 10500 – 7800 years BP, followed by an increase in precipitation in both records following 7800 years BP (Figure 5e). These changes were interpreted to reflect a relatively weak SHWW influence during the Early Holocene followed by a strengthening of the SHWW influence during the middle and late Holocene, which is consistent with Saunders et al. (2018; Figure 5e and f).

The timing of inferred changes in the SHWW are not zonally consistent, suggesting regional variability. In the eastern Pacific Ocean in New Zealand (43°S, 171°E), progressive glacier retreat and southward shift in the ITCZ and SHWW occur between ~9800 and ~6900 years ago, suggesting a warming early Holocene (Putnam et al., 2012). Whereas in South America, the changes located at Lago Condorito and Lago Guanaco suggest southward migration starting at the earliest at 7800 years ago. While southern South America might suggest a relatively linear change in the SHWW (Figure 5e) this does not negate a non-linear shift in the SHWW belt in other regions. The offset between these two records would suggest zonal variability across the Pacific, in agreement with (Kaplan et al., 2016).

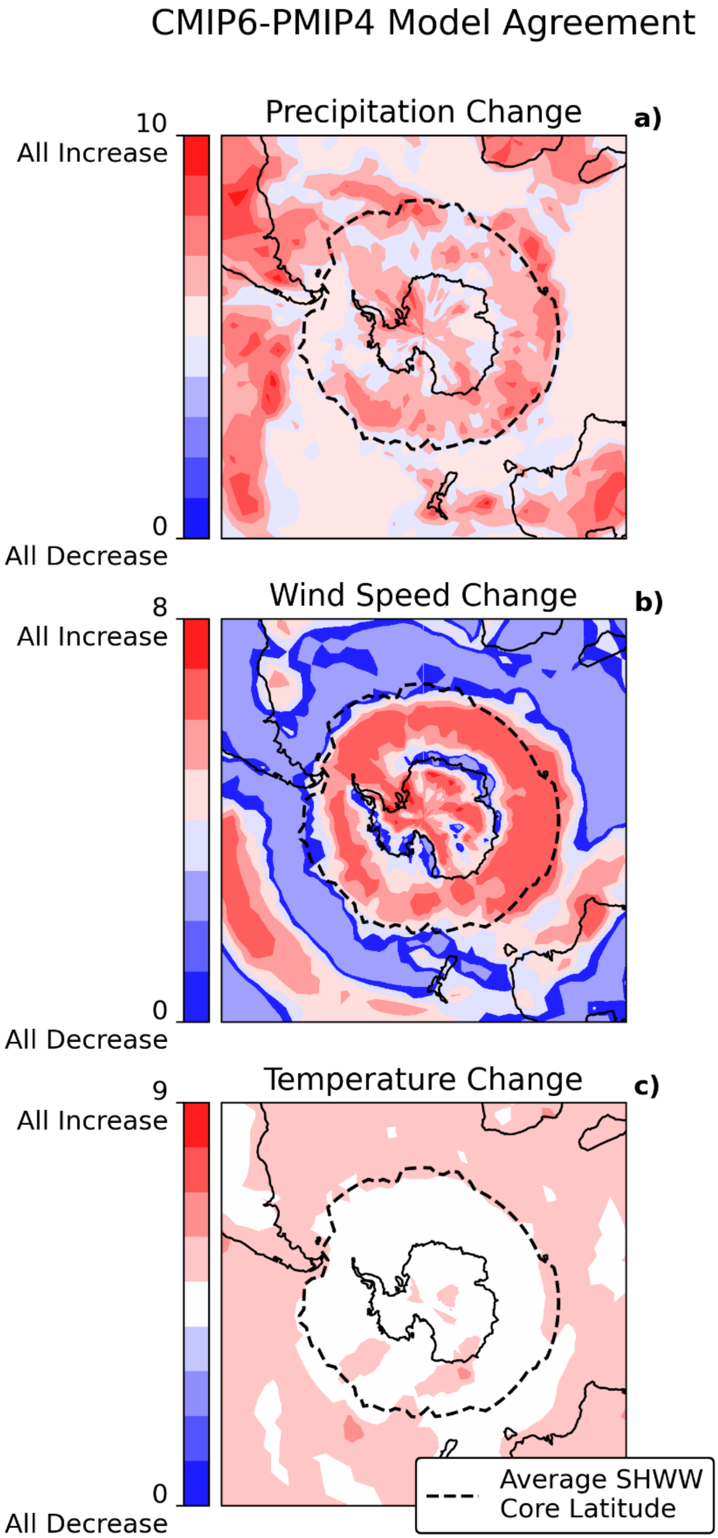
CMIP6-PMIP4 Model Agreement
Precipitation Change
a)
10
All Increase
0
All Decrease
Wind Speed Change
b)
8
All Increase
0
All Decrease
Temperature Change
c)
9
All Increase
0
All Decrease
Average SHWW
Core Latitude

Figure 4a – c: CMIP6-PMIP4 models agreement displaying difference between mid-Holocene and piControl precipitation (4a), wind speed(4b), and temperature (4c; Otto-Bliesner et al., 2017; Brierley et al., 2020). The color bar indicates the number of models that infer a positive or no/negative change in each variable between 6000 years BP and during the Pre-Industrial. Red regions indicate a stronger model consensus towards an increase and blue indicates a consensus towards a decrease in the respective variable. Values in the middle represent a lack of consensus. The black dotted line represents the average position of peak surface wind speed for both time periods.

4.3 Changes in SPC14 dust concentration and hydrologic conditions

From 7000 – 3000 years BP, South Pole dust concentration decreased by ~60% (Table S1). While we have shown this decrease is qualitatively consistent with a reduction in Patagonian surface winds, possibly related to SHWW variability (<~51°S; Figure 5a), increased precipitation in the remote dust source regions (Figure 4 and Figure 5d and e; Tonello et al., 2009; Moreno et al., 2010) or during transport may also have contributed to this change. Precipitation in Patagonian source regions is closely related to changes in surface wind speed on the Andes western slope with an opposing pattern between wind speed and precipitation on the eastern slope, due to increasing cyclonic activity and the presence of the mountains causing a rain shadow effect (Berman et al., 2012; Moreno et al., 2010; Garreaud, 2007). Precipitation trends in South America vary across regions north and south during the Holocene with icefields in Patagonia (47 – 48°S, 73.4° W) and Andes experiencing arid conditions during the early (9400 – 6300 cal years BP) and late (2400 – 1600 cal years BP) Holocene, while regions in Southern Patagonia (~50°S; ~72°W) received increased precipitation during the mid-late Holocene (Glasser et al., 2004; Tonello et al., 2009; Figure 4d; Moreno et al., 2010). However, both regions show increased in precipitation during the mid-Holocene (~7000- >3000 cal years BP; Figure 4d; Glasser et al., 2004; Tonello et al., 2009; Moreno et al., 2010; Bamonte et al., 2015). At lower latitudes (~44°S), there was a relative increase in effective moisture during the Holocene (~9500 - 4200 years BP; De Porras et al., 2014). We note that the CMIP6-PIMP4 output models suggest a broad increase in precipitation over most of South America, with disagreement in the models over the southern South America (Figure 3c). Paleoproxy lake records (Figure 5) also support a progressive increase in precipitation throughout the Holocene suggesting southward migration of the SHWW belt.

Modelled and paleoproxy increases in precipitation are also observed with increases in *Nothofagus* compared to grassland vegetation cover (Figure 4e; i.e., Moreno et al., 2010). The increase in vegetation cover and precipitation can reduce soil erosion and dust entrainment, while increasing dust fallout (i.e., Mahowald et al., 2005; Tegen and Schepanski, 2018).

Therefore, the Holocene decrease in South Pole dust may not merely be related to a southward migration of the SHWW away from the dust sources, but also to a rise in precipitation resulting from this shift that also suppressed dust mobilization.

4.4 Antarctic ice sheet thinning and CPP increase

Previous studies have linked CPP variability with changes in air mass advection and/or activation of local dust sources (Delmonte et al., 2020; Koffman et al., 2014; Albani et al., 2012; Wegner et al., 2012; Aarons et al., 2017; Gabrielli et al., 2010). We explore the changes in the SPC14 CPP within the context of the coarse particle concentration. The coarse particle concentration has a similar trend throughout the Holocene as the total particle concentration, suggesting predominantly similar dynamics between coarse and total particle concentration change. However, because the CPP increases throughout the Holocene there must be an additional forcing mechanism(s) acting upon the coarse particles.

The increase in SPC14 CPP begins ~8000 – 6000 yr B.P. (Figure 1 and 4a) coinciding with the timing of glacial retreat and dust source exposure in lower-elevation regions of Antarctica between ~7500 – 6000 yr B.P. (Figure 5h; Jones et al., 2020; Jones et al., 2015; Stutz et al., 2021; Stone et al., 2003; Hein et al., 2016; Kawamata et al., 2020). For consistency, we recalibrate ^{10}Be surface exposure ages using production rates from Putnam et al. (2010) and Kaplan et al. (2011; Supplementary S1). Newly exposed source areas in the Weddell Sea sector are plausible origins of dust in SPC14 given prevailing low-level wind patterns (Lazzara et al., 2012; Winski et al., 2021; Clem et al., 2020). However, because the South Pole has multiple air sources, either moving into the East Antarctic plateau via in the Weddell Sea (Winski et al., 2021; Clem et al., 2020; Lazzara et al., 2012) or across West Antarctica (Nicolas and Bromwich, 2011), we interpret the changes in coarse particles to reflect broader scale Antarctic changes rather than to indicate activation of a specific local source (Figure 2).

Holocene icesheet thinning, leading to exposure of Antarctic dust sources, is primarily related to 1) ocean warming (Jones et al., 2020; Stutz et al., 2021), 2) change in glacial flow patterns (Hein et al., 2016), and/or 3) reduced buttressing (Stutz et al., 2021). Strengthening and/or southward latitudinal shifts in the SHWW have been shown to increase surface upwelling of relatively warmer circumpolar deep water (CDW) and increase air mass incursions driven by cyclogenesis into the Antarctic plateau (Hillenbrand et al., 2017; Carrasco et al., 2003). It seems likely that contracting, southward shifting, and accelerating SHWW, leading to warming ocean and atmosphere, is linked to the mid-Holocene glacial retreat (i.e., Albani et al., 2012; Koffman et al., 2014) and would increase Antarctic dust sources and the increase in CPP observed in SPC14, however, the coarse dust concentration has a slight decrease and a strong running correlation until ~4000 years BP, suggesting a similar dust source and/or dynamics, which could indicate either 1) deflation of local Antarctic dust sources, similar to Holocene dynamics at Talos Dome (i.e., Albani et al., 2012) or 2) transport from mid-latitudinal sources (Adebiyi and Kok, 2020). As further evidence, the timing of decreasing surface elevation around Antarctica corresponds to increases in SPC14 CPP as a southward shift in the Atlantic ITCZ, representing warming of the Southern Hemisphere relative to the Northern Hemisphere and the Lago Guanaco which was interpreted to reflect latitudinal migrations in the SHWW (Figure 4a, c, and e; Haug et al., 2001; Moreno et al., 2010; respectively). We suggest the CPP increase is primarily related to changes in remote dust contributions in the mid-latitudinal regions and also secondarily related to Antarctic dust source deflation.

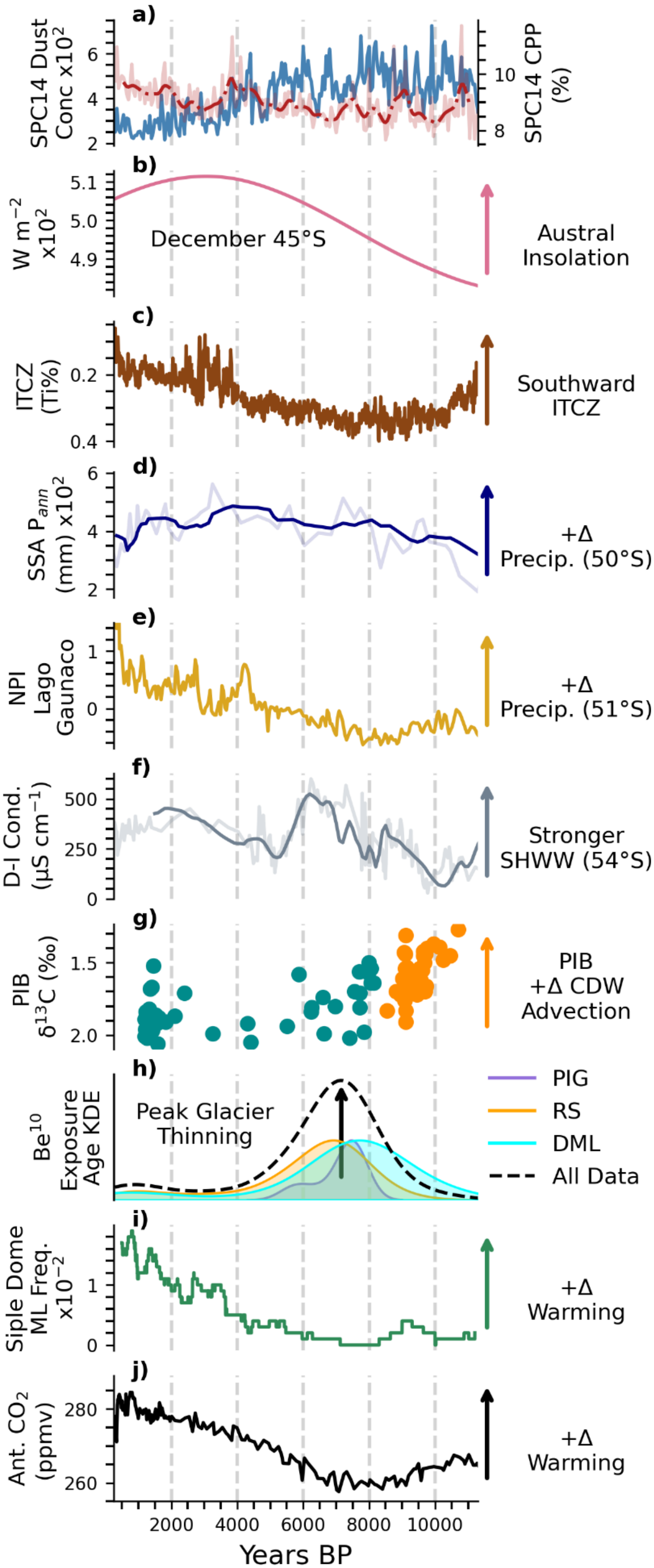

a)
SPC14 Dust Conc x10^2
SPC14 CPP (%)
b)
W m^{-2} x10^2
December 45°S
Austral Insolation
c)
ITCZ (Ti%)
Southward ITCZ
d)
SSA P$_{ann}$ (mm) x10^2
+Δ Precip. (50°S)
e)
NPI Lago Gaunaco
+Δ Precip. (51°S)
f)
D-I Cond. (μS cm^{-1})
Stronger SHWW (54°S)
g)
PIB δ^{13}C (‰)
PIB +Δ CDW Advection
h)
Be^{10} Exposure Age KDE
Peak Glacier Thinning
PIG
RS
DML
All Data
i)
Siple Dome ML Freq. x10^{-2}
+Δ Warming
j)
Ant. CO$_2$ (ppmv)
+Δ Warming
Years BP

Figure 5. Southern Hemisphere perspective of climate variability (11300 – 250 years BP). Figure a – j are stacks of different proxies spanning from the ITCZ to the South Pole. 5a) is the SPC14 dust concentration (blue; # mL^{-1}) and CPP (light red shading) and CPP 11-point rolling mean (dashed red line; %). 5b) summer (December) insolation at 45ºS (Laskar et al., 2004), 5c) Cariaco Basin Ti% (Haug et al., 2001), 5d) Cerro Frias southern Patagonia precipitation reconstruction (Tonello et al., 2009), 5e) Lago Guanaco precipitation reconstruction from Torres del Paine (Moreno et al., 2010), 5f) Macquarie Island (South Pacific) diatom-inferred (D-I) conductivity measurements interpreted to reflect relative wind strength over the island (~55°S; Saunders et al., 2018), 5g) Pine Island Bay (PIB) $\delta^{13}C$ reflective of circumpolar deep water (CDW) advection, 5h) ^{10}Be surface exposure from the Pine Island Glacier (Johnson et al., 2014), Ross Sea (Jones et al., 2020; Jones et al., 2015), and Dronning Maud Land (Kawamata et al., 2020). Scaling of each distribution kernel density estimate (KDE) is altered to show relative timing rather than magnitude of exposure dates, 5i) Siple Dome melt layer frequency record (1000-year running mean; Das and Alley, 2008), and 5j) compiled Antarctic CO_2 (Bereiter et al., 2015).

4.5 Southern Hemisphere Westerly Winds and Holocene climate

There is evidence indicating that the poleward shift in Holocene SHWW we infer at the South Pole is related to broader, hemisphere-scale changes in temperature and orbital changes. Mid-to-high latitude Southern Hemisphere Holocene proxy records provide ample evidence for an orbitally-driven southward shift of Holocene thermal gradients resulting in the strengthening of the SHWW. South Pole dust concentrations and CPP have significant relationships ($r = -0.76$ and 0.52, respectively, $p < 0.01$) with the composite Antarctic CO_2 record throughout the SPC14 Holocene record (Figure 5j). Moreno et al. (2010) interpreted the close relationship between Antarctic CO_2 and their NPI record at Lago Guanaco (Figure 5e) as a metric of southward migration of the SHWW and strengthening of the wind belt. The close relationship between the SPC14 dust concentration and CPP with Antarctic CO_2 bolsters our interpretations of southward migration of the SHWW during the Holocene. SHWW model and proxy-based latitudinal reconstructions suggest that the latitudinal position and/or strength can reflect changes in regional temperature variability over millennial to centennial timescales (i.e., Jiang and Yan, 2020; Thompson and Solomon, 2002; Toggweiler et al., 2006). High-latitude zonally averaged Holocene temperature reconstructions (60 – 90°S latitude) differ, where Kaufman et al. (2020) identify a relatively stable Holocene temperature of 0.04 ± 0.22 Δ°C (slope = < 0.01 Δ°C kyr^{-1}; relative to pre-industrial temperature) whereas Osman et al. (2021) suggest a more insolation-like increase (slope = 0.11 Δ°C kyr^{-1}; relative to last two millennia). The insolation-like structure in the South Pole dust record seems most consistent with the reconstruction of Osman et al. (2021).

Together, the data suggest that high-southern latitude wind dynamics and resulting precipitation changes are driven by high-latitude hemispheric temperature change on orbital timescales. While there is broad agreement among many proxy records, the Pine Island Bay upwelling record shows a different pattern, with reduced wind-driven upwelling near West

Antarctica after ~8 ka (Figure 5g; Hillenbrand et al., 2017). Zonal differences in wind strength may account for these apparently conflicting observations (Kaplan et al., 2016).

Opportunities for future research include describing the asymmetry in the timing of SHWW wind shifts between Western and Eastern Antarctica, which could influence the output of ocean derived CO_2 to the atmosphere. Our results further suggest the early Holocene may be a poor analogue for modern climate change. The SHWW southward shift and CO_2 transfer from the ocean to the atmosphere increased throughout the Holocene and has continued to increase today (Menviel et al., 2023). Identifying and examining WAIS stability within the context of Holocene changes therefore becomes critical if the early Holocene can no longer be used as an analogue to modern temperature change.

5 Conclusions

The SPC14 record over the course of the Holocene documents a decrease in dust concentration accompanied by an increase in the proportion of coarse particles (i.e., CPP). We interpret these trends as reflecting; 1) a linear southward shift in SHWW during the mid-Holocene leading to decreasing surface wind speeds and increasing precipitation affecting fine dust mobilization and transport in the mid-latitudes and 2) increased Antarctic wind strength and temperature associated with a southward shift in SHWW, leading to marginal ice retreat and exposure of local dust sources. Together the timing and structure of these changes are consistent with an orbitally driven southward shift of the SHWW and global temperature belts. The interpreted shifts in the SHWW are coeval with changes in the ITCZ, suggesting that over millennial time scales, the SHWW are driven by Southern Hemisphere temperature change modulated by earth's orbital characteristics and rising CO_2.

Data Availability

Dust datasets used in this paper are available at the U.S. Antarctic Program Data Center (DOI: 10.15784/601553.).

Author Contributions

AC analyzed the data and prepared the manuscript with contributions from all co-authors. KK, EO, JCD, and MW designed the experiments and guided the overall research effort. DF and ZT melted the core and measured the Abakus data and collected discrete samples. KA wrote the Abakus cleaning code. DW and BK provided data analysis and writing support. AP provided writing support. MH provided laboratory analysis feedback.

Competing Interests

The authors declare that they have no conflicts of interest.

Acknowledgements

This research was funded by the US National Science Foundation grants [1443336 (Osterberg); 1443397 (Kreutz); 1443663 (Cole-Dai); and 1443105, 1141839 (Steig)]. We thank Mark Twickler, Joseph Souney and the South Pole Ice Core (SPICEcore) Science Coordination Office for administering the project; the U.S. Ice Drilling Program for support activities through NSF Cooperative Agreement 1836328; the 109th New York Air National Guard for airlift in Antarctica; the field team who helped collect the core; the members of South Pole station who facilitated the field operations; the National Science Foundation Ice Core Facility for ice core processing; and the many student researchers involved in producing the data used in this research. The authors gratefully acknowledge the NOAA Air Resources Laboratory (ARL) for the provision of the HYSPLIT transport and dispersion model and/or READY website (https://www.ready.noaa.gov) used in this publication. We acknowledge the World Climate Research Programme, which, through its Working Group on Coupled Modelling, coordinated and promoted CMIP6. We thank the climate modelling groups for producing and making available their model output, the Earth System Grid Federation (ESGF) for archiving the data and providing access, and the multiple funding agencies who support CMIP6 and ESGF. CMIP6 and PMIP4 model data was retrieved from the World Data Center for Climate (hosted by DKRZ) and Lawrence Livermore. We thank two anonymous reviewers, whose thoughtful suggestions and questions served to clarify and improve the paper.

References

Aarons, S. M., Aciego, S. M., McConnell, J. R., Delmonte, B., and Baccolo, G.: Dust Transport to the Taylor Glacier, Antarctica, During the Last Interglacial, Geophysical Research Letters, 46, 2261-2270, 10.1029/2018GL081887, 2019.

Aarons, S. M., Aciego, S. M., Gabrielli, P., Delmonte, B., Koornneef, J. M., Wegner, A., and Blakowski, M. A.: The impact of glacier retreat from the Ross Sea on local climate: Characterization of mineral dust in the Taylor Dome ice core, East Antarctica, Earth and Planetary Science Letters, 444, 34-44, 10.1016/j.epsl.2016.03.035, 2016.

Aarons, S. M., Aciego, S. M., Arendt, C. A., Blakowski, M. A., Steigmeyer, A., Gabrielli, P., Sierra-Hernández, M. R., Beaudon, E., Delmonte, B., Baccolo, G., May, N. W., and Pratt, K. A.: Dust composition changes from Taylor Glacier (East Antarctica) during the last glacial-interglacial transition: A multi-proxy approach, Quaternary Science Reviews, 162, 60-71, 10.1016/j.quascirev.2017.03.011, 2017.

Adebiyi, A. A. and Kok, J. F.: Climate models miss most of the coarse dust in the atmosphere, Science Advances, 6, eaaz9507, doi:10.1126/sciadv.aaz9507, 2020.

Albani, S., Balkanski, Y., Mahowald, N., Winckler, G., Maggi, V., and Delmonte, B.: Aerosol-Climate Interactions During the Last Glacial Maximum, Current Climate Change Reports, 4, 99-114, 10.1007/s40641-018-0100-7, 2018.

Albani, S., Delmonte, B., Maggi, V., Baroni, C., Petit, J. R., Stenni, B., Mazzola, C., and Frezzotti, M.: Interpreting last glacial to Holocene dust changes at Talos Dome (East Antarctica): implications for atmospheric variations from regional to hemispheric scales, Climate of the Past, 8, 741-750, 10.5194/cp-8-741-2012, 2012.

Anderson, R. F., Ali, S., Bradtmiller, L. I., Nielsen, S. H. H., Fleisher, M. Q., Anderson, B. E., and Burckle, L. H.: Wind-Driven Upwelling in the Southern Ocean and the Deglacial Rise in Atmospheric CO_2, Science, 323, 1443-1448, 10.1126/science.1167441, 2009.

Arimoto, R., Zeng, T., Davis, D., Wang, Y., Khaing, H., Nesbit, C., and Huey, G.: Concentrations and sources of aerosol ions and trace elements during ANTCI-2003, Atmospheric Environment, 42, 2864-2876, 10.1016/j.atmosenv.2007.05.054, 2008.

Bamonte, F. P., Mancini, M. V., Sottile, G. D., Marcos, M. A., and Gogorza, C.: Vegetation dynamics from Lago San Martín area (Southwest Patagonia, Argentina) during the last 6,500 years, Vegetation History and Archaeobotany, 24, 267-277, 10.1007/s00334-014-0473-z, 2015.

Bereiter, B., Eggleston, S., Schmitt, J., Nehrbass-Ahles, C., Stocker, T. F., Fischer, H., Kipfstuhl, S., and Chappellaz, J.: Revision of the EPICA Dome C CO_2 record from 800 to 600 kyr before present, Geophysical Research Letters, 42, 542-549, 10.1002/2014GL061957, 2015.

Berman, A. L., Silvestri, G., and Compagnucci, R.: Eastern Patagonia Seasonal Precipitation: Influence of Southern Hemisphere Circulation and Links with Subtropical South American Precipitation, Journal of Climate, 25, 6781-6795, https://doi.org/10.1175/JCLI-D-11-00514.1, 2012.

Bodhaine, B. A., Deluisi, J. J., Harris, J. M., Houmere, P., and Bauman, S.: Aerosol measurements at the South Pole, Tellus B: Chemical and Physical Meteorology, 38, 223-235, 10.3402/tellusb.v38i3-4.15131, 1986.

Breton, D. J., Koffman, B. G., Kurbatov, A. V., Kreutz, K. J., and Hamilton, G. S.: Quantifying Signal Dispersion in a Hybrid Ice Core Melting System, Environmental Science & Technology, 46, 11922-11928, 10.1021/es302041k, 2012.

Brierley, C. M., Zhao, A., Harrison, S. P., Braconnot, P., Williams, C. J. R., Thornalley, D. J. R., Shi, X., Peterschmitt, J. Y., Ohgaito, R., Kaufman, D. S., Kageyama, M., Hargreaves, J. C., Erb, M. P., Emile-Geay, J., D'Agostino, R., Chandan, D., Carré, M., Bartlein, P. J., Zheng, W., Zhang, Z., Zhang, Q., Yang, H., Volodin, E. M., Tomas, R. A., Routson, C., Peltier, W. R., Otto-Bliesner, B., Morozova, P. A., McKay, N. P., Lohmann, G., Legrande, A. N., Guo, C., Cao, J., Brady, E., Annan, J. D., and Abe-Ouchi, A.: Large-scale features and evaluation of the PMIP4-CMIP6 midHolocene simulations, Clim. Past, 16, 1847-1872, 10.5194/cp-16-1847-2020, 2020.

Carrasco, J. F., Bromwich, D. H., and Monaghan, A. J.: Distribution and Characteristics of Mesoscale Cyclones in the Antarctic: Ross Sea Eastward to the Weddell Sea, Monthly Weather Review, 131, 289-301, 10.1175/1520-0493(2003)131<0289:dacomc>2.0.co;2, 2003.

Casey, K. A., Fudge, T. J., Neumann, T. A., Steig, E. J., and Cavitte, M. G. P.: The 1500 m South Pole ice core: recovering a 40 ka environmental record, Annals of glaciology, 55, 137-146, 10.3189/2014AoG68A016, 2014.

Chesler, A., Winski, D., Kreutz, K., Koffman, B., Osterberg, E., Ferris, D., Thundercloud, Z., Mohan, J., Cole-Dai, J., Wells, M., Handley, M., Putnam, A., Anderson, K., and Harmon, N.: Non-spherical microparticle shape in Antarctica during the last glacial period affects dust volume-related metrics, Clim. Past, 19, 477-492, 10.5194/cp-19-477-2023, 2023.

Clem, K. R., Fogt, R. L., Turner, J., Lintner, B. R., Marshall, G. J., Miller, J. R., and Renwick, J. A.: Record warming at the South Pole during the past three decades, Nature Climate Change, 10, 762-770, 10.1038/s41558-020-0815-z, 2020.

Das, S. B. and Alley, R. B.: Rise in frequency of surface melting at Siple Dome through the Holocene: Evidence for increasing marine influence on the climate of West Antarctica, Journal of Geophysical Research: Atmospheres, 113, 10.1029/2007JD008790, 2008.

de Porras, M. E., Maldonado, A., Quintana, F. A., Martel-Cea, A., Reyes, O., and Méndez, C.: Environmental and climatic changes in central Chilean Patagonia since the Late Glacial (Mallín El Embudo, 44° S), Clim. Past, 10, 1063-1078, 10.5194/cp-10-1063-2014, 2014.

Delmonte, B., Petit, J., and Maggi, V.: Glacial to Holocene implications of the new 27000-year dust record from the EPICA Dome C (East Antarctica) ice core, Climate Dynamics, 18, 647-660, 10.1007/s00382-001-0193-9, 2002.

Delmonte, B., Baroni, C., Andersson, P. S., Narcisi, B., Salvatore, M. C., Petit, J. R., Scarchilli, C., Frezzotti, M., Albani, S., and Maggi, V.: Modern and Holocene aeolian dust variability from Talos Dome (Northern Victoria Land) to the interior of the Antarctic ice sheet, Quaternary Science Reviews, 64, 76-89, 10.1016/j.quascirev.2012.11.033, 2013.

Delmonte, B., Winton, H., Baroni, M., Baccolo, G., Hansson, M., Andersson, P., Baroni, C., Salvatore, M. C., Lanci, L., and Maggi, V.: Holocene dust in East Antarctica: Provenance and variability in time and space, The Holocene, 30, 546-558, 10.1177/0959683619875188, 2020.

Denton, G. H., Putnam, A. E., Russell, J. L., Barrell, D. J. A., Schaefer, J. M., Kaplan, M. R., and Strand, P. D.: The Zealandia Switch: Ice age climate shifts viewed from Southern Hemisphere moraines, Quaternary Science Reviews, 257, 106771, 10.1016/j.quascirev.2020.106771, 2021.

Gabrielli, P., Wegner, A., Petit, J. R., Delmonte, B., and De Deckker, P.: A major glacial-interglacial change in aeolian dust composition inferred from Rare Earth Elements in Antarctic ice, Quaternary science reviews, 29, 265-273, 10.1016/j.quascirev.2009.09.002, 2010.

Garreaud, R.: Precipitation and Circulation Covariability in the Extratropics, Journal of Climate, 20, 4789-4797, https://doi.org/10.1175/JCLI4257.1, 2007.

Glasser, N. F., Harrison, S., Winchester, V., and Aniya, M.: Late Pleistocene and Holocene palaeoclimate and glacier fluctuations in Patagonia, Global and Planetary Change, 43, 79-101, 10.1016/j.gloplacha.2004.03.002, 2004.

Harris, J. M.: An analysis of 5-day midtropospheric flow patterns for the South Pole: 1985-1989, Tellus B: Chemical and Physical Meteorology, 10.3402/tellusb.v44i4.15466, 1992.

Haug, G. H., Hughen, K. A., Sigman, D. M., Peterson, L. C., and Röhl, U.: Southward Migration of the Intertropical Convergence Zone Through the Holocene, Science, 293, 1304-1308, 10.1126/science.1059725, 2001.

Hein, A. S., Marrero, S. M., Woodward, J., Dunning, S. A., Winter, K., Westoby, M. J., Freeman, S. P. H. T., Shanks, R. P., and Sugden, D. E.: Mid-Holocene pulse of thinning in the Weddell Sea sector of the West Antarctic ice sheet, Nature Communications, 7, 12511, 10.1038/ncomms12511, 2016.

Hillenbrand, C.-D., Smith, J. A., Hodell, D. A., Greaves, M., Poole, C. R., Kender, S., Williams, M., Andersen, T. J., Jernas, P. E., Elderfield, H., Klages, J. P., Roberts, S. J., Gohl, K., Larter, R. D., and Kuhn, G.: West Antarctic Ice Sheet retreat driven by Holocene warm water incursions, Nature, 547, 43-48, 10.1038/nature22995, 2017.

Hogan, A., Kebschull, K., Townsend, R., Murphey, B., Samson, J., and Barnard, S.: Particle concentrations at the South Pole, on meteorological and climatological time scales; Is the difference important?, Geophysical Research Letters, 11, 850-853, 10.1029/GL011i009p00850, 1984.

Jiang, N. X. and Yan, Q.: Evolution of the meridional shift of the subtropical and subpolar westerly jet over the Southern Hemisphere during the past 21,000 years, Quaternary Science Reviews, 246, 10.1016/j.quascirev.2020.106544, 2020.

Johnson, J. S., Bentley, M. J., Smith, J. A., Finkel, R. C., Rood, D. H., Gohl, K., Balco, G., Larter, R. D., and Schaefer, J. M.: Rapid Thinning of Pine Island Glacier in the Early Holocene, Science, 343, 999-1001, doi:10.1126/science.1247385, 2014.

Jones, R. S., Whitmore, R. J., Mackintosh, A. N., Norton, K. P., Eaves, S. R., Stutz, J., and Christl, M.: Regional-scale abrupt Mid-Holocene ice sheet thinning in the western Ross Sea, Antarctica, Geology, 49, 278-282, 10.1130/g48347.1, 2020.

Jones, R. S., Mackintosh, A. N., Norton, K. P., Golledge, N. R., Fogwill, C. J., Kubik, P. W., Christl, M., and Greenwood, S. L.: Rapid Holocene thinning of an East Antarctic outlet glacier driven by marine ice sheet instability, Nature Communications, 6, 8910, 10.1038/ncomms9910, 2015.

Kaplan, M. R., Schaefer, J. M., Strelin, J. A., Denton, G. H., and Anderson, R. F.: Patagonian and southern South Atlantic view of Holocene climate, Quaternary science reviews, 141, 112-125, 10.1016/j.quascirev.2016.03.014, 2016.

Kaplan, M. R., Strelin, J. A., Schaefer, J. M., Denton, G. H., Finkel, R. C., Schwartz, R., Putnam, A. E., Vandergoes, M. J., Goehring, B. M., and Travis, S. G.: In-situ cosmogenic 10Be production rate at Lago Argentino, Patagonia: Implications for late-glacial climate chronology, Earth and Planetary Science Letters, 309, 21-32, 10.1016/j.epsl.2011.06.018, 2011.

Kaufman, D., McKay, N., Routson, C., Erb, M., Dätwyler, C., Sommer, P. S., Heiri, O., and Davis, B.: Holocene global mean surface temperature, a multi-method reconstruction approach, Scientific Data, 7, 201, 10.1038/s41597-020-0530-7, 2020.

Kawamata, M., Suganuma, Y., Doi, K., Misawa, K., Hirabayashi, M., Hattori, A., and Sawagaki, T.: Abrupt Holocene ice-sheet thinning along the southern Soya Coast, Lützow-Holm Bay, East Antarctica, revealed by glacial geomorphology and surface exposure dating, Quaternary Science Reviews, 247, 106540, 10.1016/j.quascirev.2020.106540, 2020.

Koffman, B. G., Kreutz, K. J., Breton, D. J., Kane, E. J., and Winski, D. A.: Centennial-scale variability of the Southern Hemisphere westerly wind belt in the eastern Pacific over the past two millennia, Climate of the past, 10, 1125-1144, 10.5194/cp-10-1125-2014, 2014.

Koffman, B. G., Goldstein, S. L., Winckler, G., Kaplan, M. R., Bolge, L., and Biscaye, P.: Abrupt Changes in Atmospheric Circulation During the Medieval Climate Anomaly and Little Ice Age Recorded by Sr-Nd Isotopes in the Siple Dome Ice Core, Antarctica, Paleoceanography and Paleoclimatology, 38, e2022PA004543, https://doi.org/10.1029/2022PA004543, 2023.

Lambert, F., Bigler, M., Steffensen, J. P., Hutterli, M., and Fischer, H.: Centennial mineral dust variability in high-resolution ice core data from Dome C, Antarctica, Clim. Past, 8, 609-623, 10.5194/cp-8-609-2012, 2012.

Lambert, F., Delmonte, B., Petit, J. R., Bigler, M., and Kaufmann, P. R.: Dust-climate couplings over the past 800,000 years from the EPICA Dome C ice core, Nature (London), 452, 616-619, 10.1038/nature06763, 2008.

Lamy, F., Kilian, R., Arz, H. W., Francois, J.-P., Kaiser, J., Prange, M., and Steinke, T.: Holocene changes in the position and intensity of the southern westerly wind belt, Nature Geoscience, 3, 695-699, 10.1038/ngeo959, 2010.

Laskar, J., Robutel, P., Joutel, F., Gastineau, M., Correia, A. C. M., and Levrard, B.: A long-term numerical solution for the insolation quantities of the Earth, A&A, 428, 261-285, doi.org/10.1051/0004-6361:20041335, 2004.

Lazzara, M. A., Keller, L. M., Markle, T., and Gallagher, J.: Fifty-year Amundsen–Scott South Pole station surface climatology, Atmospheric Research, 118, 240-259, doi.org/10.1016/j.atmosres.2012.06.027, 2012.

Mahowald, N. M., Baker, A. R., Bergametti, G., Brooks, N., Duce, R. A., Jickells, T. D., Kubilay, N., Prospero, J. M., and Tegen, I.: Atmospheric global dust cycle and iron inputs to the ocean, Global Biogeochemical Cycles, 19, doi.org/10.1029/2004GB002402, 2005.

Markle, B. R., Steig, E. J., Roe, G. H., Winckler, G., and McConnell, J. R.: Concomitant variability in high-latitude aerosols, water isotopes and the hydrologic cycle, Nature Geoscience, 11, 853-859, 10.1038/s41561-018-0210-9, 2018.

Menviel, L. C., Spence, P., Kiss, A. E., Chamberlain, M. A., Hayashida, H., England, M. H., and Waugh, D.: Enhanced Southern Ocean CO2 outgassing as a result of stronger and poleward shifted southern hemispheric westerlies, Biogeosciences, 20, 4413-4431, 10.5194/bg-20-4413-2023, 2023.

Moreno, P. I., Francois, J. P., Moy, C. M., and Villa-Martínez, R.: Covariability of the Southern Westerlies and atmospheric CO_2 during the Holocene, Geology, 38, 727-730, 10.1130/g30962.1, 2010.

Nicolas, J. P. and Bromwich, D. H.: Climate of West Antarctica and Influence of Marine Air Intrusions, Journal of Climate, 24, 49-67, 10.1175/2010jcli3522.1, 2011.

Osman, M. B., Tierney, J. E., Zhu, J., Tardif, R., Hakim, G. J., King, J., and Poulsen, C. J.: Globally resolved surface temperatures since the Last Glacial Maximum, Nature, 599, 239-244, 10.1038/s41586-021-03984-4, 2021.

Osterberg, E. C., Handley, M. J., Sneed, S. B., Mayewski, P. A., and Kreutz, K. J.: Continuous ice core melter system with discrete sampling for major ion, trace element, and stable isotope analyses, Environmental Science & Technology, 40, 3355-3361, 10.1021/es052536w, 2006.

Otto-Bliesner, B. L., Braconnot, P., Harrison, S. P., Lunt, D. J., Abe-Ouchi, A., Albani, S., Bartlein, P. J., Capron, E., Carlson, A. E., Dutton, A., Fischer, H., Goelzer, H., Govin, A., Haywood, A., Joos, F., LeGrande, A. N., Lipscomb, W. H., Lohmann, G., Mahowald, N., Nehrbass-Ahles, C., Pausata, F. S. R., Peterschmitt, J. Y., Phipps, S. J., Renssen, H., and Zhang, Q.: The PMIP4 contribution to CMIP6 – Part 2: Two interglacials, scientific objective and experimental design for Holocene and Last Interglacial simulations, Geosci. Model Dev., 10, 3979-4003, 10.5194/gmd-10-3979-2017, 2017.

Parungo, F., Bodhaine, B., and Bortniak, J.: Seasonal variation in antarctic aerosol, Journal of Aerosol Science, 12, 491-504, 10.1016/0021-8502(81)90052-5, 1981.

Perren, B. B., Hodgson, D. A., Roberts, S. J., Sime, L., Van Nieuwenhuyze, W., Verleyen, E., and Vyverman, W.: Southward migration of the Southern Hemisphere westerly winds corresponds with warming climate over centennial timescales, Communications Earth & Environment, 1, 58, 10.1038/s43247-020-00059-6, 2020.

Petit, J. R., Mourner, L., Jouzel, J., Korotkevich, Y. S., Kotlyakov, V. I., and Lorius, C.: Palaeoclimatological and chronological implications of the Vostok core dust record, Nature, 343, 56-58, 1990.

Potenza, M. A. C., Albani, S., Delmonte, B., Villa, S., Sanvito, T., Paroli, B., Pullia, A., Baccolo, G., Mahowald, N., and Maggi, V.: Shape and size constraints on dust optical properties from the Dome C ice core, Antarctica, Scientific Reports, 6, 9, 10.1038/srep28162, 2016.

Putnam, A. E., Schaefer, J. M., Denton, G. H., Barrell, D. J. A., Finkel, R. C., Andersen, B. G., Schwartz, R., Chinn, T. J. H., and Doughty, A. M.: Regional climate control of glaciers in New Zealand and Europe during the pre-industrial Holocene, Nature Geoscience, 5, 627-630, 10.1038/ngeo1548, 2012.

Putnam, A. E., Schaefer, J. M., Barrell, D. J. A., Vandergoes, M., Denton, G. H., Kaplan, M. R., Finkel, R. C., Schwartz, R., Goehring, B. M., and Kelley, S. E.: In situ cosmogenic ^{10}Be production-rate calibration from the Southern Alps, New Zealand, Quaternary Geochronology, 5, 392-409, 10.1016/j.quageo.2009.12.001, 2010.

Rolph, G., Stein, A., and Stunder, B.: Real-time Environmental Applications and Display sYstem: READY, Environmental Modelling & Software, 95, 210-228, https://doi.org/10.1016/j.envsoft.2017.06.025, 2017.

Russell, J. L., Dixon, K. W., Gnanadesikan, A., Stouffer, R. J., and Toggweiler, J. R.: The Southern Hemisphere Westerlies in a Warming World: Propping Open the Door to the Deep Ocean, Journal of Climate, 19, 6382-6390, 10.1175/jcli3984.1, 2006.

Saunders, K. M., Roberts, S. J., Perren, B., Butz, C., Sime, L., Davies, S., Van Nieuwenhuyze, W., Grosjean, M., and Hodgson, D. A.: Holocene dynamics of the Southern Hemisphere westerly winds and possible links to CO2 outgassing, Nature Geoscience, 11, 650-655, 10.1038/s41561-018-0186-5, 2018.

Schwanck, F., Simões, J. C., Handley, M., Mayewski, P. A., Auger, J. D., Bernardo, R. T., and Aquino, F. E.: A 125-year record of climate and chemistry variability at the Pine Island Glacier ice divide, Antarctica, The Cryosphere, 11, 1537-1552, 10.5194/tc-11-1537-2017, 2017.

Sheridan, P., Andrews, E., Schmeisser, L., Vasel, B., and Ogren, J.: Aerosol Measurements at South Pole: Climatology and Impact of Local Contamination, Aerosol and Air Quality Research, 16, 855-872, 10.4209/aaqr.2015.05.0358, 2016.

Simonsen, M. F., Cremonesi, L., Baccolo, G., Bosch, S., Delmonte, B., Erhardt, T., Kjær, H. A., Potenza, M., Svensson, A., and Vallelonga, P.: Particle shape accounts for instrumental discrepancy in ice core dust size distributions, Clim. Past Discuss., 19 (in press), 2018.

Stein, A. F., Draxler, R. R., Rolph, G. D., Stunder, B. J. B., Cohen, M. D., and Ngan, F.: NOAA's HYSPLIT Atmospheric Transport and Dispersion Modeling System, Bulletin of the American Meteorological Society, 96, 2059-2077, https://doi.org/10.1175/BAMS-D-14-00110.1, 2015.

Stone, J. O., Balco, G. A., Sugden, D. E., Caffee, M. W., Sass, L. C., Cowdery, S. G., and Siddoway, C.: Holocene Deglaciation of Marie Byrd Land, West Antarctica, Science, 299, 99-102, 2003.

Stutz, J., Mackintosh, A., Norton, K., Whitmore, R., Baroni, C., Jamieson, S. S. R., Jones, R. S., Balco, G., Salvatore, M. C., Casale, S., Lee, J. I., Seong, Y. B., McKay, R., Vargo, L. J., Lowry, D., Spector, P., Christl, M., Ivy Ochs, S., Di Nicola, L., Iarossi, M., Stuart, F., and Woodruff, T.: Mid-Holocene thinning of David Glacier, Antarctica: chronology and controls, The Cryosphere, 15, 5447-5471, 10.5194/tc-15-5447-2021, 2021.

Sugden, D. E., McCulloch, R. D., Bory, A. J. M., and Hein, A. S.: Influence of Patagonian glaciers on Antarctic dust deposition during the last glacial period, Nature geoscience, 2, 281-285, 10.1038/ngeo474, 2009.

Tegen, I. and Schepanski, K.: Climate Feedback on Aerosol Emission and Atmospheric Concentrations, Current Climate Change Reports, 4, 1-10, 10.1007/s40641-018-0086-1, 2018.

Thompson, D. W. J. and Solomon, S.: Interpretation of Recent Southern Hemisphere Climate Change, Science, 296, 895-899, doi:10.1126/science.1069270, 2002.

Toggweiler, J. R. and Russell, J.: Ocean circulation in a warming climate, Nature, 451, 286-288, 2008.

Toggweiler, J. R., Russell, J. L., and Carson, S.: Midlatitude westerlies, atmospheric CO_2, and climate change during the ice ages, Paleoceanography, 21, n-a, 2006.

Tonello, M. S., Mancini, M. V., and Seppä, H.: Quantitative reconstruction of Holocene precipitation changes in southern Patagonia, Quaternary Research, 72, 410-420, 10.1016/j.yqres.2009.06.011, 2009.

van der Bilt, W. G. M., D'Andrea, W. J., Oppedal, L. T., Bakke, J., Bjune, A. E., and Zwier, M.: Stable Southern Hemisphere westerly winds throughout the Holocene until intensification in the last two millennia, Communications Earth & Environment, 3, 186, 10.1038/s43247-022-00512-8, 2022.

Varma, V., Prange, M., Merkel, U., Kleinen, T., Lohmann, G., Pfeiffer, M., Renssen, H., Wagner, A., Wagner, S., and Schulz, M.: Holocene evolution of the Southern Hemisphere westerly winds in transient simulations with global climate models, Clim. Past, 8, 391-402, 10.5194/cp-8-391-2012, 2012.

Vecchio, M. A., Costas-Rodríguez, M., Caiazzo, L., Bruschi, F., Hobin, K., Vanhaecke, F., and Grotti, M.: Provenance of mineral dust deposited on Antarctica over the last sixty years by strontium isotopic analysis of snow from Dome C, Atmospheric Environment, 338, 120850, https://doi.org/10.1016/j.atmosenv.2024.120850, 2024.

Wegner, A., Gabrielli, P., Wilhelms-Dick, D., Ruth, U., Kriews, M., De Deckker, P., Barbante, C., Cozzi, G., Delmonte, B., and Fischer, H.: Change in dust variability in the Atlantic sector of Antarctica at the end of the last deglaciation, Clim. Past, 8, 135-147, 10.5194/cp-8-135-2012, 2012.

Winski, D. A., Osterberg, E. C., Kreutz, K. J., Ferris, D. G., Cole-Dai, J., Thundercloud, Z., Huang, J., Alexander, B., Jaeglé, L., Kennedy, J. A., Larrick, C., Kahle, E. C., Steig, E. J., and Jones, T. R.: Seasonally Resolved Holocene Sea Ice Variability Inferred From South Pole Ice Core Chemistry, Geophysical Research Letters, 48, e2020GL091602, 10.1029/2020GL091602, 2021.

Winski, D. A., Fudge, T. J., Ferris, D. G., Osterberg, E. C., Fegyveresi, J. M., Cole-Dai, J., Thundercloud, Z., Cox, T. S., Kreutz, K. J., Ortman, N., Buizert, C., Epifanio, J., Brook, E. J., Beaudette, R., Severinghaus, J., Sowers, T., Steig, E. J., Kahle, E. C., Jones, T. R., Morris, V., Aydin, M., Nicewonger, M. R., Casey, K. A., Alley, R. B., Waddington, E. D., Iverson, N. A., Dunbar, N. W., Bay, R. C., Souney, J. M., Sigl, M., and McConnell, J. R.: The SP19 chronology for the South Pole Ice Core – Part 1: volcanic matching and annual layer counting, Clim. Past, 15, 1793-1808, 10.5194/cp-15-1793-2019, 2019.

Zwier, M., van der Bilt, W. G., de Stigter, H., and Bjune, A. E.: Pollen evidence of variations in Holocene climate and Southern Hemisphere Westerly Wind strength on sub-Antarctic South Georgia, The Holocene, 32, 147-158, 10.1177/09596836211060495, 2022.